



**HAL**  
open science

# Three-dimensional paraxial migration method without lateral splitting

Michel Kern

► **To cite this version:**

Michel Kern. Three-dimensional paraxial migration method without lateral splitting. *Mathematical Methods in Geophysical Imaging III*, 1995, San Diego, United States. 10.1117/12.218504. hal-01316193

**HAL Id: hal-01316193**

**<https://inria.hal.science/hal-01316193>**

Submitted on 15 May 2016

**HAL** is a multi-disciplinary open access archive for the deposit and dissemination of scientific research documents, whether they are published or not. The documents may come from teaching and research institutions in France or abroad, or from public or private research centers.

L'archive ouverte pluridisciplinaire **HAL**, est destinée au dépôt et à la diffusion de documents scientifiques de niveau recherche, publiés ou non, émanant des établissements d'enseignement et de recherche français ou étrangers, des laboratoires publics ou privés.



Distributed under a Creative Commons Attribution 4.0 International License

# A 3D paraxial migration method without lateral splitting

M. Kern

INRIA, Domaine de Voluceau-Rocquencourt, BP 105, F-78153 Le Chesnay Cédex

## ABSTRACT

We introduce a migration algorithm based on paraxial wave equation that does not use any splitting in the lateral variables. The discretization is first derived in the constant coefficient case by higher order finite differences, then generalized to arbitrarily varying velocities via finite elements. We present a detailed plane wave analysis in a homogeneous medium, and give evidence that numerical dispersion and anisotropy can be controlled. Propagation along depth is done with a higher order method based on a conservative Runge Kutta method. At each step in depth we have to solve a large linear system. This is the most time consuming part of the method. The key to obtaining good performance lies in the use of a Conjugate Gradient like iterative solver. We show the performance of the method with a model example.

**Keywords:** Seismic migration, paraxial equations, finite difference, finite element, numerical dispersion, iterative methods.

## 1 INTRODUCTION

Finite difference migration provides an efficient and accurate migration method. Its chief advantage is to allow for arbitrary variation of the velocity. For 3D situations, the main drawback is the relatively high cost of the method. To overcome this drawback, several authors<sup>10,12,18</sup> have advocated using splitting in the lateral directions, so as to implement 3D migration at a cost proportional to the number of grid points. This would not be true if one did not use splitting and solved the linear system by a direct method. Of course splitting introduces errors, mainly along the diagonal directions, so corrections have to be added, in a mostly ad-hoc fashion. Alternatively, Collino and Joly<sup>6</sup> have proposed a *consistent* splitting method, that is one in which isotropy error is at the level of numerical error.

This paper details the implementation of a migration algorithm based on paraxial equations whose main feature is that it deals directly with the 2D lateral equation, without resorting to any splitting in the lateral variables. We are still able to maintain efficiency by solving the large linear system at each step in depth by modern iterative methods, since convergence is rapid as soon as the frequency is not too low. Further highlights of the paper are:

- Use of higher order schemes in both the lateral and the transverse variables, in order to obtain high accuracy;
- Precise control of dispersion and anisotropy in a homogeneous medium by plane wave analysis;
- Extension to arbitrarily heterogeneous media via finite elements.

An outline of the paper is as follow: We begin by recalling the derivation of paraxial equations, and give a variational formulation for the particular choice we make in this paper. We then describe the discretization in the lateral variables, first in the constant velocity case, then in the variable velocity case. We present the procedure for back-propagation in depth, and detail how we solve the linear system. We conclude by presenting a numerical example.

## 2 PARAXIAL EQUATIONS

Paraxial equations are PDEs intended to approximate the up-going part of the solution of the wave equation. As is well known, an approximation is needed since this up-going wave is actually represented (in the frequency - wave-number domain) by a non-rational function. There is a large literature on paraxial approximations, but we will just refer to the companion paper<sup>3</sup> for references. In this paper we use approximations coming from Bamberger and al.,<sup>1</sup> and for ease of exposition concentrate on the so called generalized 45° equation (it is shown in<sup>3</sup> how the general case can be reduced to this one) :

$$\begin{cases} \frac{\partial \tilde{v}}{\partial z} = \frac{i\omega}{c} \tilde{v} - \frac{i\omega}{c} \beta \tilde{\psi} \\ \frac{\omega}{c} \tilde{\psi} + \alpha \operatorname{div}(c \nabla \tilde{\psi}) = -\operatorname{div}(c \nabla \tilde{v}). \end{cases} \quad (1)$$

where  $c$  is the (position dependent) velocity,  $\tilde{v}$  is related to  $u$  (the up-going solution) by  $u = \sqrt{c} \tilde{v}$ , and  $\omega$  is the frequency.  $\tilde{\psi}$  is an auxiliary unknown introduced in order to avoid higher order derivatives.

Equation (1) has been shown in<sup>1</sup> to be a proper generalization of the classical 45° equation. By choosing values for the parameters  $\alpha$  and  $\beta$  one obtains several approximations, valid over different ranges of angles. Choosing  $\alpha = 0, \beta = 1/2$  gives the 15° approximation, whereas for  $\alpha = 1/4, \beta = 1/2$  one obtains the 45° approximation.

After the classical Claerbout<sup>4</sup> change of function  $v = \tilde{v} e^{i\omega/cz}$  (and the corresponding change for  $\tilde{\psi}$ ), which enables us to take vertical propagation exactly into account, we introduce a bounded domain  $\Omega = [-L, L]^2 \times [0, Z]$ , where  $L$  and  $Z$  are “large” numbers, and apply appropriate boundary conditions on the fictitious lateral boundary. It is shown in<sup>15</sup> that by using first order boundary conditions, one obtains a decrease of energy. For the problem posed in the bounded domain, we can give a variational formulation. We set:

$$\begin{cases} m(u, v) = \int_{\Omega} \frac{u \bar{v}}{c} dx dy, \\ a(u, v) = \int_{\Omega} c \nabla u \nabla \bar{v} dx dy + i\omega \int_{\Gamma} u \bar{v} d\gamma. \end{cases} \quad (2)$$

then the variational formulation of equation( 1) is:

Find  $v, \psi$  such that

$$\begin{cases} \frac{d}{dz}(v, w) = -i\omega \beta m(\psi, w) & \forall w \\ -\omega^2 m(\psi, \varphi) + a(\alpha \psi + v, \varphi) = 0 & \forall \varphi \\ v(z = 0) = v^0 \text{ given.} \end{cases} \quad (3)$$

Of course, one should make functional spaces precise. This is done in.<sup>15</sup> Our discretization procedure will be based on (3).

### 3 DISCRETIZATION IN THE LATERAL VARIABLES

In this section we describe our main discretization procedure. We begin with the homogeneous medium case, as it lends itself to a complete dispersion analysis, and we later generalize it to take into account heterogeneous media.

In both cases, we will use a square uniform grid of size  $h$ . Of course in the variable coefficient case this is not necessary, but it is current practice, it is convenient, and it helps maintain some control over the numerical anisotropy.

#### 3.1 Homogeneous medium

In this section, we disregard boundary conditions, so that we can apply plane wave analysis later on. In this case, we can base our discretization of (8) on finite differences. Indeed, we define approximations to the Laplace operator, and (we explain why we do this below) to the identity by:

$$\begin{cases} \Delta_\gamma^h = \gamma \Delta_1^h + (1 - \gamma) \Delta_0^h \\ M_{\mu, \nu}^h = I + \frac{h^2}{12} (\mu \Delta_1^h + \nu \Delta_0^h) \end{cases} \quad (4)$$

where  $(\gamma, \mu, \nu)$  are 3 real parameters and where:

$$\begin{cases} -(\Delta_1^h u)_{ij} = \frac{1}{h^2} (-u_{i,j-1} - u_{i-1,j} - u_{i+1,j} - u_{i,j+1} + 4u_{i,j}) \\ -(\Delta_0^h u)_{ij} = \frac{1}{2h^2} (-u_{i-1,j-1} - u_{i+1,j-1} - u_{i-1,j+1} - u_{i+1,j+1} + 4u_{i,j}). \end{cases} \quad (5)$$

In other words,  $\Delta_\gamma^h$  is a nine points approximation to the Laplacian, second order for any value of  $\gamma$ , and that respects the basic symmetries of the mesh. Also  $M_{\mu, \nu}^h$  is a nine points approximation to the identity, second order for all values of  $\mu$  and  $\nu$ . As shown below, introducing these two parameters will give us some additional freedom in controlling numerical anisotropy.

The discrete version of our problem is now:

$$\begin{cases} \frac{\partial v_h}{\partial t^2} = -\frac{i\omega}{c} \beta \psi_h \\ \frac{\omega^2}{c^2} M_{\mu, \nu}^h \psi_h + \alpha \Delta_\gamma^h \psi_h = -\Delta_\gamma^h v_h. \end{cases} \quad (6)$$

We need to explain why we approximate the identity in two different ways. When we eliminate  $\psi_h^n$  in (6) above, we do not want to invert a matrix. Thus we keep the mass matrix in the first equation as the identity (or a diagonal mass matrix in the next subsection). On the other hand, the dispersion analysis that follows will show the usefulness of introducing  $M_{\mu, \nu}^h$ . The main drawback will become apparent when we deal with heterogeneous media in the next subsection, as we are not able to prove any stability estimate for the discrete problem.

#### 3.2 Heterogeneous media

The schemes described in the previous subsection are extended to heterogeneous media via a special choice of finite elements on a regular grid. This enables us to recover the finite difference method when the medium is homogeneous. In order to preserve isotropy, we define 3 meshes on the square grid, named after the finite element

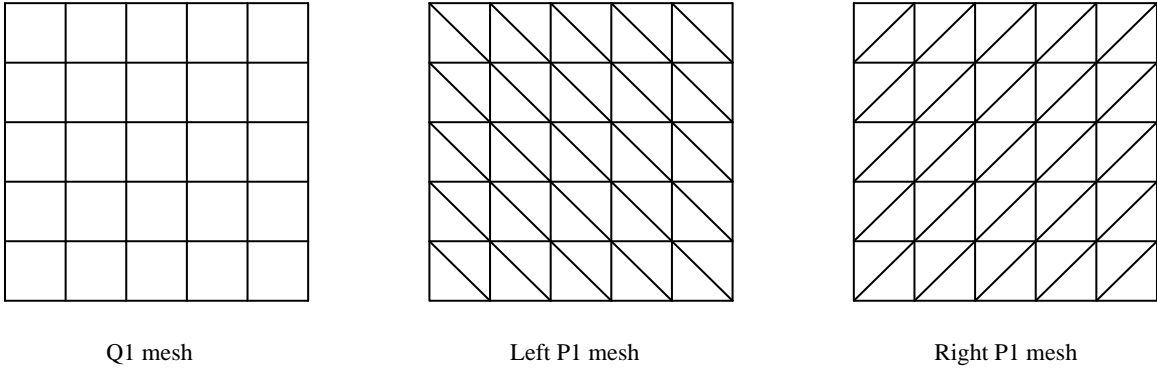


Figure 1: The three meshes

they lead to: a left P1 mesh, a right P1 mesh, and a Q1 mesh. By looking at figure 1 the names should be self-explanatory.

We now define the various matrices that will provide the discrete form of (3). We let

- $M^Q$  be the Q1 consistent mass matrix;
- $M^P$  be the average of the consistent right and left P1 mass matrices;
- $M^*$  be the lumped Q1 mass matrix;
- $K^Q$  be the Q1 stiffness matrix;
- $K^P$  be the P1 stiffness matrix;

then we set

$$\begin{cases} M_{\mu,\nu} = (1 - \frac{\mu + \nu}{2})M^* + \frac{3}{2}(\mu - \nu)M^Q + (2\nu - \mu)M^P, \\ K_\gamma = \frac{3}{2}K^Q + \frac{1}{2}(3\gamma - 1)K^P, \end{cases}$$

The reason for the strange looking coefficients is again that we want to recover the finite difference scheme of the previous section when the medium is homogeneous. This choice is explained in more details in.<sup>15</sup>

The semi-discrete problem is now: Find  $v_h \in V_h$ , such that

$$\begin{cases} \frac{dv_h}{dz} = -i\omega\beta M^* \psi_h \\ -\omega^2 M_{\mu,\nu} \psi_h + K_\gamma(\alpha\psi_h + v_h) = 0 \\ v_h(z = z^n) = v^n. \end{cases} \quad (7)$$

The reason we introduce both consistent and lumped mass matrices is that we need to invert  $M^*$  when we eliminate  $\psi$ , so we want to keep it diagonal. On the other hand, we need to the consistent version of  $M_{\mu,\nu}$  to recover accuracy and isotropy as shown in the previous section.

To conclude this section, let us note that detailed computations of the matrices can be found in Kern.<sup>16</sup>

### 3.3 Discretization in depth

Equation (2) is formally similar to a Schrödinger's equation, and it is known that most explicit schemes for Schrödinger's equation are unconditionally unstable. Thus we turn toward implicit schemes. The most widely used is perhaps the mid-point rule as it insures conservation of a discrete energy

$$\begin{cases} \frac{v_h^{n+1} - v_h^n}{\Delta z} = -i\omega\beta M^* \psi_h^n \\ -\omega^2 M_{\mu,\nu} \psi_h^n + \alpha K_\gamma (\alpha\psi + \frac{v^{n+1} + v^n}{2}) = 0 \end{cases} \quad (8)$$

where  $v_h^n$  denotes an approximation of  $v_h$  at depth  $n\Delta z$ . This is a second order method

In Joly and Kern,<sup>14</sup> we derived a fourth order scheme, which turned out to be identical to the fourth order 2-steps Runge Kutta method (it can also be obtained as a fourth order diagonal Padé approximant to the exponential function). It has the same conservative character as the second order scheme. But non-conservative schemes can also be useful, as they remove unwanted components of the wavefronts.<sup>5</sup> Kern<sup>16</sup> introduced non-conservative variants of the second and fourth order schemes that are first and third order respectively. The first order one is none other than the well-know  $\theta$  scheme. They are both based on rational fraction to the exponential<sup>17</sup>

$$\begin{cases} R_1(x, \theta) = \frac{1 - i(1 - \theta)x}{1 + i\theta x} \\ R_2(x, \theta) = \frac{1 - i(1 - \theta)/2x - (1/3 - \theta)/4x^2}{1 + i(1 + \theta)/2x - (1/3 + \theta)/4x^2} \end{cases} \quad (9)$$

The mid-point rule is recovered from  $R_1$  for  $\theta = 1/2$ , while  $R_2$  gives the fourth order scheme for  $\theta = 0$ .

As explained by Kern,<sup>16</sup> a simple and efficient implementation can be based on factoring the rational fraction  $R_2$  as

$$R_2(x, \theta) = \frac{(1 - i\sigma_1 x)(1 - i\sigma_2 x)}{(1 + i\tau_1 x)(1 + i\tau_2 x)} \quad (10)$$

(the exact expressions for  $\sigma_i$  and  $\tau_i$  are unimportant). Then, the third and fourth order schemes can just be implemented as two stages of the first order method (see<sup>16</sup> for details).

At each step in depth, we can eliminate  $\psi_h^n$ , and then have to solve one or two linear systems of the form

$$S(v_h^{n+1} - v_h^n) = i\omega\beta\Delta z(\sigma - \tau)K_\gamma v_h^n \quad (11)$$

where

$$S = (\alpha K_\gamma - \omega^2 M_{\mu,\nu})M^{*-1} - i\omega\beta\Delta z\tau K_\gamma.$$

## 4 PLANE WAVE ANALYSIS

We now return to the setting of section 3.1, and perform a plane wave analysis, that is we look for solutions to (6) of the form:

$$v_h^n(i, j) = \exp i(ik_x h + jk_y h + n\Delta z k_z).$$

Such solutions can only exist if  $(k_x, k_y, k_z)$  satisfy what is known as the *discrete dispersion relation*. In Joly and Kern<sup>14</sup> it is shown that if we let  $k_z = \frac{\omega}{c} + k_z^1$  (Claerbout's change of variables) the dispersion relation can be written as

$$\frac{2}{\Delta z} \tan \frac{k_z^1 \Delta z}{2} = F_{\gamma,\mu,\nu}(k, h) \quad (12)$$

for the second order (in depth) scheme, and

$$\frac{2}{\Delta z} \tan \frac{k_z^1 \Delta z}{2} = F_{\gamma, \mu, \nu}(k, h) \left( 1 - \frac{1}{12} F_{\gamma, \mu, \nu}(k, h)^2 \right)^{-1} \quad (13)$$

for the fourth order scheme, where

$$F_{\gamma, \mu, \nu}(k, h) = -\frac{\omega}{c} \frac{\beta D_\gamma(k, h)}{\frac{\omega^2}{c^2} M_{\mu, \nu}(k, h) - \alpha D_\gamma(k, h)} \quad (14)$$

and where  $D_\gamma$  and  $M_{\mu, \nu}$  are the *symbols* of  $\Delta_\gamma^h$  and  $M_{\mu, \nu}^h$  respectively. Precise expressions are given in the above reference.

From the dispersion we can make several deduction concerning properties of our scheme:

**Accuracy** From a Taylor expansion of (12) one can see that the scheme is always second order with respect to  $h$ . Conditions for it to be fourth order in the lateral variables are  $\gamma = 2/3, \mu + \nu = 1$ .<sup>14</sup> The first condition is natural. It just says that we are using the so-called Arakawa scheme. The second condition is the justification for the introduction of the parameters  $\mu$  and  $\nu$ . Without them, we cannot achieve fourth order.

**Stability** Since  $k_z$  is always real, the scheme is conservative, and in particular unconditionally stable.. Of course this is only true because of our idealized hypotheses (no boundary, constant velocity). In the general case, the best we can hope for is dissipativity.

**Isotropy** For no choice of  $\mu, \nu$  can we obtain a sixth order scheme, but we can try and make the error as isotropic as possible. This can be achieved for  $\mu = 8/15, \nu = 7/15$ , giving a “maxi-isotropic” scheme.

**Vertical propagation** Because of Claerbout’s change of variable, vertical propagation is exact. Thus, for  $k_x = k_y = 0$ , we have  $k_z = \omega/c$ .

The clearest way to assess the influence of the several parameters entering our schemes is via a numerical comparison of the dispersion error. We use a criterion devised by Collino<sup>5</sup> in 2D, based on the dip angle error, which is  $\arctan\left(\frac{|k|}{k_z}\right)$ . Thus we compare this quantity for the exact paraxial equation, and that for the approximate one. Note that we use the paraxial equation, and not the (arguably more relevant) wave equation, as we have no way of justifying the latter. We send in a plane wave coming in at an angle  $\theta$  with the vertical, and  $\varphi$  with the  $x$  axis in the horizontal plane. By making all quantities dimension-less, we see that the relevant parameters can be chosen as:

- The (tangent of the) angle of the incoming plane wave with the vertical,  $p = \tan \theta$ ;
- The (inverse of the) number of points per wavelength in the horizontal direction,  $H = \omega h / 2\pi c$ ;
- The ration of the step sizes in  $z$  to that in  $(x, y)$ ,  $b = \Delta z / h$ ;

There are too many parameters in sight. We keep  $\alpha = 1/4$  and  $\beta = 1/2$  fixed (we chose a particular paraxial equation), and also keep  $b = 1$  (it was shown in<sup>14</sup> that for the most interesting schemes, the influence of  $b$  is small). In the next figures, we plot the dip error angle as a function of either  $H$ ,  $\varphi$  or both , for different values of the scheme parameters  $\gamma, \mu, \nu$  and the second or fourth order in depth scheme.

In figures 2 and 3, we compare the second and fourth order schemes in the lateral variables, while remaining second order in depth. Figure 2 plots the dip error angle as a function of  $H$  and  $\varphi$ , while figure 3 keeps  $\varphi = \pi/4$  as this is the worst case. The superiority of the fourth-order scheme is self evident.

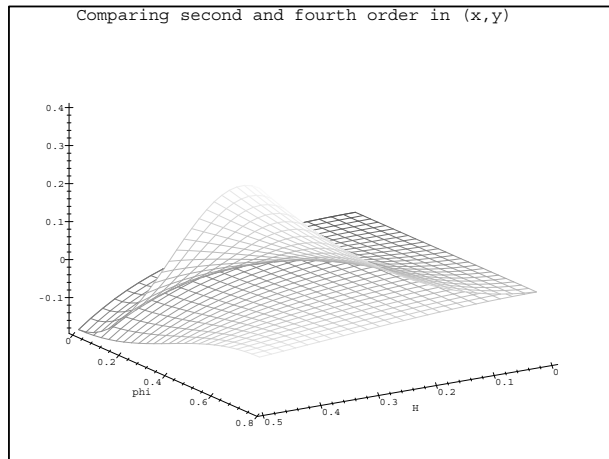


Figure 2: Comparing the second and fourth order schemes in  $(x, y)$ . Top surface: second order, bottom surface fourth order.

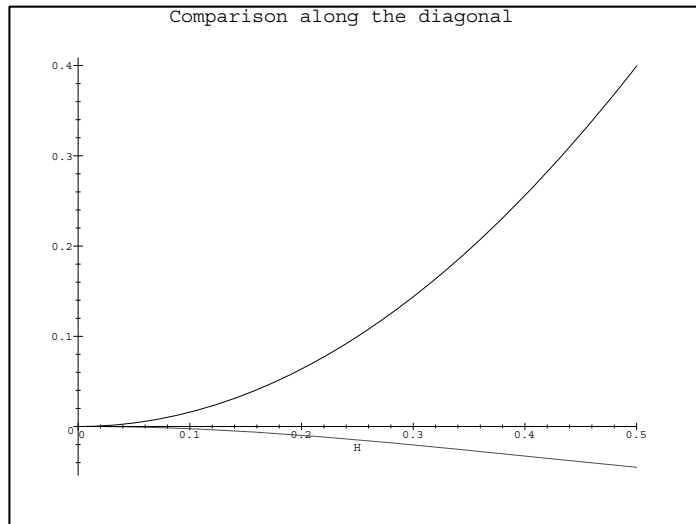


Figure 3: Comparing the second and fourth order schemes in  $(x, y)$ . Same as previous figure, with  $\varphi = \pi/4$ .

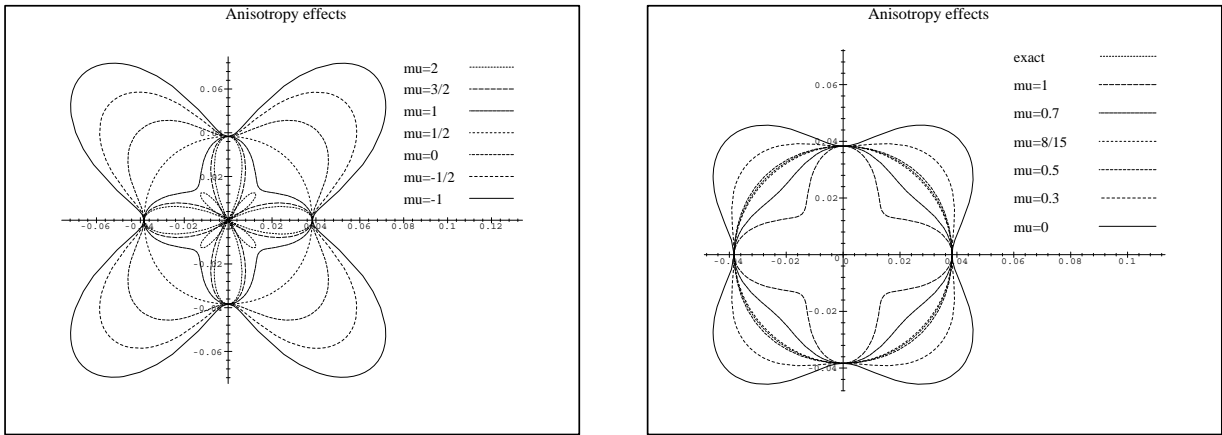


Figure 4: Anisotropy error (polar plot, for  $H = 0.3$  and varying values of  $\mu$ ).

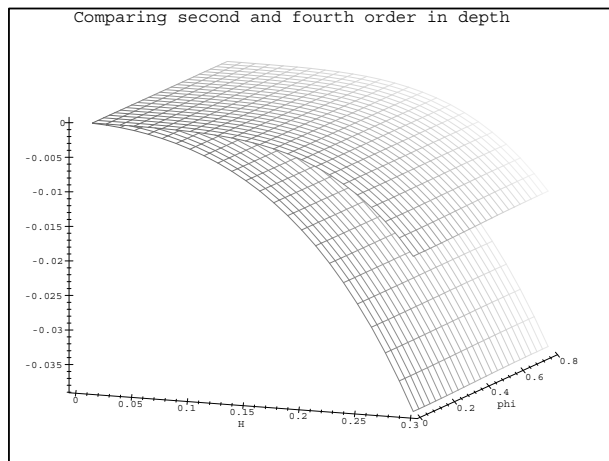


Figure 5: Comparing the second and fourth order schemes in depth. Top surface: fourth order, bottom surface: second order.

We now keep  $\gamma$  fixed at  $2/3$ , and investigate the influence of the  $\mu, \nu$  parameters on isotropy, subject to  $\mu + \nu = 1$ . Figure 4 shows polar plots of the dip error angle as a function of  $\varphi$ , for  $H = 0.3$ , and several values of  $\mu$ . The isotropy error appears to be quite insensitive to the precise value of  $\mu$  around the “maxi-isotropic” value. We note also that a value of  $\mu$  outside of  $[0, 1]$  might be interesting: in,<sup>14</sup> we noted that  $\mu = 16/15$  has the property to minimize the  $L^2$  norm of the error over all angles.

Eventually, in figure 5, we compare the schemes for evolution in depth. Again the higher order scheme obviously has better properties.

## 5 SOLUTION OF THE LINEAR SYSTEM

System (11) will usually be large. In the example presented below, the grid is  $100 \times 100$ . More realistic cases would have 3 times this resolution. The main reason why most authors use lateral splitting is precisely to avoid having to solve this system. We now show how this task can be carried out at a reasonable cost. The matrix  $S$  is very sparse, as it has only 9 non-zero diagonals. Thus we solve the system by iterative methods. For symmetric positive definite systems the (preconditioned) conjugate gradient algorithm is currently considered as the method of choice.<sup>11</sup> Unfortunately, our system is complex and non-hermitian, which renders its solution more difficult. Indeed, no bulletproof method exists for such systems, even though this is an area of active research.<sup>8</sup> Among the most successful methods, let us quote

**GMRES**<sup>19</sup> This is probably the most robust method, as it minimizes the residual at each iteration. For unsymmetric matrices this can only be done by explicitly remembering all previous search directions, so this method has the drawback of requiring a large amount of memory.

**BCG**<sup>7</sup> It is the simplest to implement. It amounts to applying the conjugate gradient method to the (non positive definite) matrix

$$\begin{bmatrix} 0 & S^* \\ S & 0 \end{bmatrix}.$$

A more theoretical derivation shows that this method is actually a Lanczos bidiagonalization,<sup>13</sup> which means that it is susceptible to breakdown: it is possible that some iterates cannot be computed. While actual breakdown are unlikely, near breakdown are quite common and manifest themselves in an erratic convergence curve.

**QMR**<sup>9</sup> This method has been designed to prevent breakdowns in the Lanczos process. It has the same low memory requirements of BCG, being based on a three term recurrence, while having a convergence theorem almost as good as that of GMRES.

We have implemented BCG and QMR, with varying results. With only diagonal preconditioning, we found the method converged rapidly (6 to 10 iterations) for all but the very few smallest frequencies. At low frequencies, up to 300 iterations could be required. This is especially troublesome since those frequencies contribute very little to the final migrated image. Several things could be done to circumvent this problem (but none of them has been implemented for lack of time): change the mesh according to the frequency. When adding the individual contributions to the migrated image, this requires some form of interpolation. Alternatively, one could use a Taylor expansion for low frequencies. Let us emphasize that this rapid convergence means that the overall cost of the method is comparable to the cost of methods that use splitting (be it the classical one as in,<sup>12</sup> or the consistent ones of<sup>6,2</sup>). It is a small multiple of the number of grid points. Thus at least for frequencies that are not too low, the method is a viable alternative to splitting.

## 6 NUMERICAL EXAMPLE

We illustrate the method with a simple numerical example. It consists of the migration of a point source in a homogeneous medium. The computational domain is 1250 m in each of the horizontal directions, and 625 m in the vertical direction. The grid sizes are  $h = \Delta z = 12.5$  m. The velocity is 1000 m/s. The source is located on the surface at the center of the computational domain, the time of the explosion is 0.5125 s (82% of the travel time to the bottom), and the frequency cutoff of the source is 50 Hz. The computations were run on a Cray C90, and took 10 minutes, running at close to 500 Mflops.

In figure 6 we compare 3 of the schemes: the second order one, the maxi-isotropic one, and the one that minimizes the mean square of the dispersion error. We show horizontal sections of the migrated image at 2 different depths. It is quite clear that both fourth order schemes have much better isotropy properties than the second order one, even though they all seem to show a comparable amount of dispersion. This is even more evident in figure 7 where we compare vertical slices of the migrated image along the  $x$  coordinate axis for the second order, and maxi-isotropic schemes. In this figure, though, what is apparent is not so much numerical dispersion as the limits of the 45° equation for angles that are close to 5°. In all cases, though numerical dispersion is kept at an acceptable level.

## 7 CONCLUSIONS

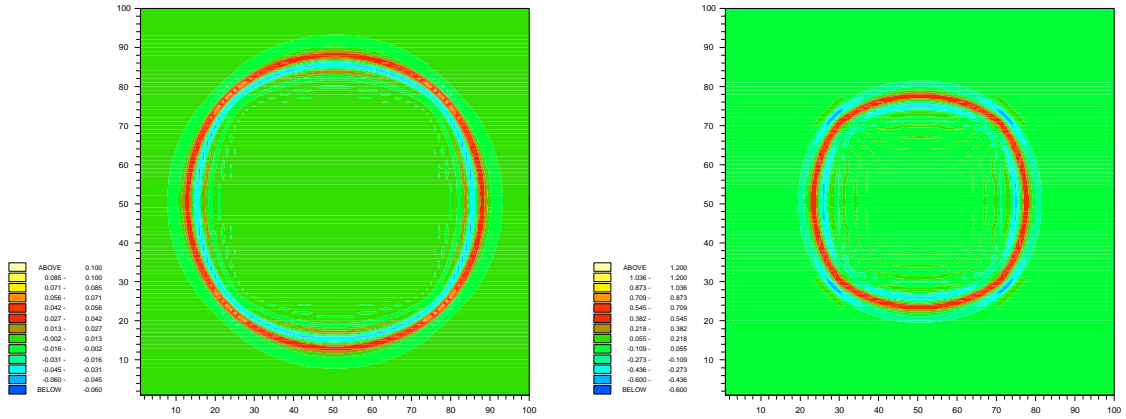
We have presented a numerical method for solving the paraxial wave equation without compromising either accuracy or isotropy. The key to achieving this goal is an efficient solution of the linear system. Although there is still need for more work at low frequencies, we have shown how the use of modern iterative methods made this feasible.

## 8 ACKNOWLEDGMENTS

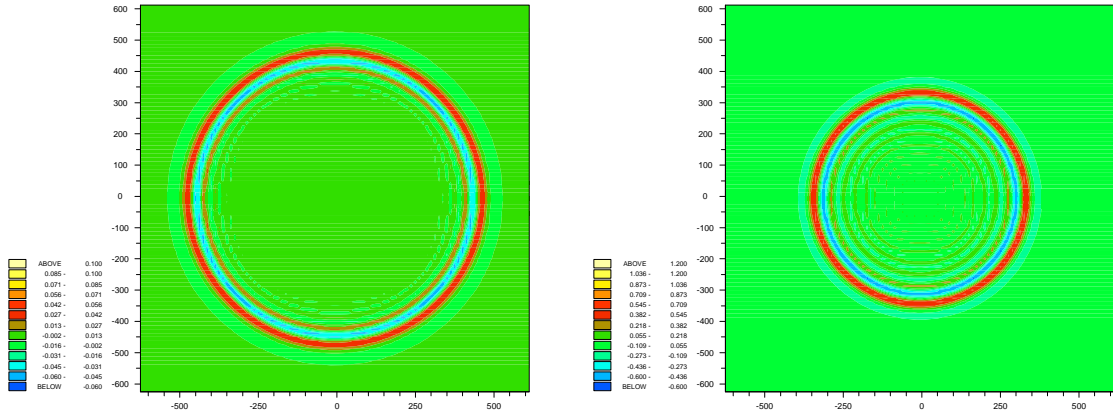
This research was carried out as part of the Prestack Structural Interpretation consortium project (PSI). The authors hereby acknowledge the support provided by the sponsors of this project. The numerical simulations were performed on the Cray C90 at IDRIS (France). It is also a pleasure to thank P. Joly, F. Collino and E. Bécache for numerous fruitful discussions.

## 9 REFERENCES

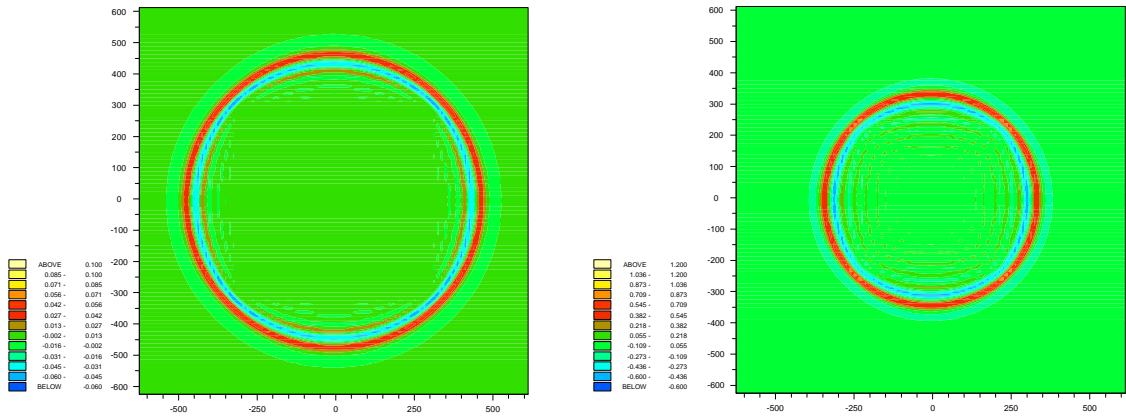
- [1] A. Bamberger, B. Engquist, L. Halpern, and P. Joly. Paraxial approximations in heterogeneous media. *SIAM Journal on Applied Mathematics*, 48:99–128, 1988.
- [2] E. Bécache, F. Collino, and P. Joly. Higher order numerical schemes for the paraxial wave equation. Yearly report, PSI Consortium, 1995.
- [3] E. Bécache, F. Collino, M. Kern, and P. Joly. On two migration methods based on paraxial equations in a 3d heterogeneous medium. In S. Hassanzadeh, editor, *Mathematical Methods in Geophysical Imaging III*. SPIE, 1995.
- [4] J. F. Claerbout. *Imaging the Earth's Interior*. Blackwell Scientific Publication Co., Oxford, 1985.



(a) Second order



(b) Fourth order, isotropic



(c) Fourth order, min dispersion

Figure 6: Comparison of 3 schemes: Top row: second order ( $\gamma = 1, \mu = 1, \nu = 0$ ), Middle row: fourth order, with isotropic error ( $\gamma = 2/3, \mu = 8/15, \nu = 7/15$ ), Bottom row: fourth order with “minimal mean dispersion” ( $\gamma = 2/3, \mu = 15/16, \nu = -1/16$ , bottom row). Left column: slice at 125 m, right column: slice at 375 m

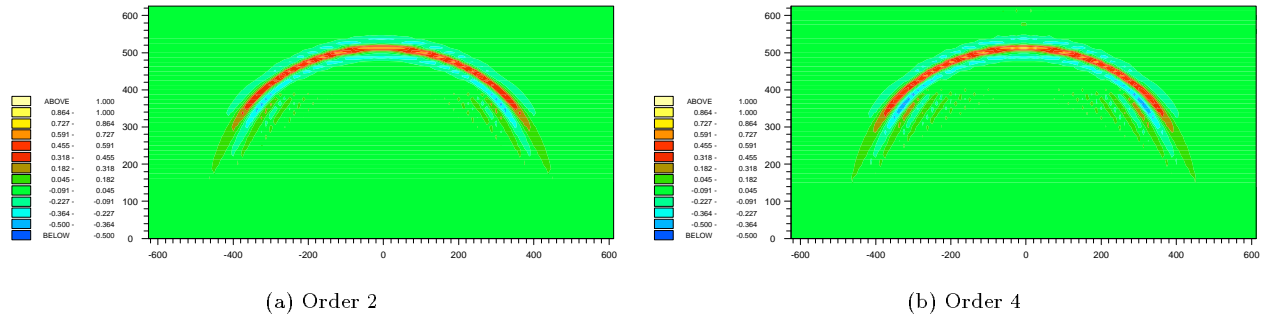


Figure 7: Vertical slices along the  $x$  axis

- [5] F. Collino. *Analyse Numérique de Modèles de Propagation d'Ondes. Application à la Migration et à l'Inversion des Données Sismiques*. PhD thesis, Université Paris IX, 1987.
- [6] F. Collino and P. Joly. Splitting of operators, alternate directions and paraxial approximations for the 3-d wave equation. *submitted to SIAM J. Sci. Comp.*, 1994.
- [7] R. Fletcher. Conjugate gradient methods for indefinite systems. In G. A. Watson, editor, *Proceedings of the Dundee Conference on Numerical Analysis – Lecture Notes in Mathematics, Vol. 506*, pages 73–89, Dundee, Scotland, 1975. Springer Verlag, Berlin.
- [8] R. W. Freund, G. H. Golub, and N. M. Nachtigal. Iterative solution of linear systems. *Acta Numerica*, 1:57–100, 1992.
- [9] R. W. Freund and N. M. Nachtigal. QMR: a quasi-minimal residual method for non-hermitian linear systems. Technical Report 90.09, RIACS, 1990.
- [10] P. Froidevaux. First results of a 3D prestack migration program. In *60th Ann. Meeting. Soc. Expl. Geophys.*, 1990.
- [11] G. H. Golub and C. F. van Loan. *Matrix Computations*. The John Hopkins University Press, second edition, 1989.
- [12] R. W. Graves and R. W. Clayton. Modeling acoustic waves with paraxial extrapolators. *Geophysics*, 55:306–319, 1990.
- [13] M. H. Gutknecht. A completed theory of the unsymmetric Lanczos process and related algorithms, part i. *SIAM J. Matrix Anal. Appl.*, 13:594–639, 1992.
- [14] P. Joly and M. Kern. Numerical methods for 3D migration. First yearly report, PSI Consortium, 1990.
- [15] M. Kern. Numerical methods for the 3D paraxial wave equation in heterogeneous media. Yearly report, PSI Consortium, 1991.
- [16] M. Kern. Numerical methods for the 3D paraxial wave equation in heterogeneous media, part iii. Yearly report, PSI Consortium, 1992.
- [17] J. D. Lambert. *Numerical Methods for Ordinary Differential Systems*. John Wiley and Sons, 1991.
- [18] Z. Li. Compensating finite-difference errors in 3D migration and modelling. *Geophysics*, 56:1650–1660, 1991.
- [19] Y. Saad and M. H. Schultz. GMRES: A generalized minimum residual algorithm for solving nonsymmetric linear systems. *SIAM J. Sci. Stat. Comp.*, 7:856–869, 1986.